

Comparison of CT enhancement patterns and histologic features in hepatocellular carcinoma up to 2 cm: Assessment of malignant potential with claudin-10 immunohistochemistry

YUICHI SANADA¹, KAZUHIRO YOSHIDA³ and HIROYUKI ITOH²

Departments of ¹Surgery and ²Medicine, Saiseikai-kure Hospital; ³Department of Surgical Oncology, Research Institution for Radiation Biology and Medicine, Hiroshima University, 1-2-3 Kasumi, Minami-ku, Hiroshima 734-8551, Japan

Received October 16, 2006; Accepted December 13, 2006

Abstract. The purpose of this study was to compare features of computed tomography (CT) and histologic features of hepatocellular carcinoma (HCC) of up to 2 cm in diameter with the immunohistochemical staining pattern of claudin-10, a recently identified prognostic factor for resected HCC. Twelve cases of resected HCC of up to 2 cm in diameter were assessed retrospectively. Preoperative dynamic CT was reviewed, and three enhancement patterns were identified. Type I (n=6) was defined as a pattern of hyperenhancement throughout the tumor in early-phase CT, decreasing to hypoenhancement in late-phase CT (high-low), a finding characteristic of HCC. Type II tumors (n=2) appeared as an area of hyperenhancement in early-phase CT, and an area of hyperenhancement in late-phase CT (low-high). Histologically, type II tumors were considered unusual types, and included combined hepatocellular-cholangiocarcinoma and scirrhous HCC. In type III tumors (n=4), high-low, low-high and low-low components were observed. Type III tumors showed multinodular-type morphology and comprised both moderately and poorly differentiated HCC with marked necrosis and fibrosis. Each nodule was divided by fibrous septa. In three of the four type III cases, recurrence occurred within 6 months after resection. Immunohistochemistry of claudin-10 showed positivity in five of the 12 cases, including four type III cases. Results of this study suggest that type III tumors have greater malignant potential than the other tumor types.

Introduction

Diagnosis of hepatocellular carcinoma (HCC) of up to 2 cm in diameter can be achieved readily by serology and radiology.

Recommendations made at the EASL conference state that HCC can be diagnosed without biopsy in patients with cirrhosis with a mass >2 cm in diameter showing characteristic arterial vascularization on triphasic CT (1). However, in HCC of up to 2 cm, preoperative early-phase CT often shows enhancement patterns other than hyperenhancement. In such cases, diagnosis of HCC can be made by clinical features and increased levels of tumor markers including α -fetoprotein and vitamin-K antagonist II. Thus, assessment of enhancement patterns on preoperative dynamic CT scan should be performed to predict the histologic features and malignant potential of tumors, including recurrences after hepatectomy (2,3). Some investigators have reported that the macroscopic subtype of multinodular type can be a predictor of prognosis and recurrence after hepatectomy. However, Hui *et al* reported that the rate of correct diagnosis of macroscopic subtype by CT is only 46% (2).

In the present study, we retrospectively reviewed the cases of 12 patients who underwent surgical resection of HCC of up to 2 cm in diameter to clarify the association between CT enhancement patterns and histopathologic features. It has been hypothesized that the differences in gross appearance, which are determined by patterns of tumor growth and spread, involve different molecular mechanisms (4). Inayoshi *et al* reported that the gross appearance of HCC reflects E-cadherin expression and can indicate early recurrence after hepatectomy (3). Recently, several proteins have been identified as prognostic factors for HCC. Of these, claudin-10, a member of the claudin tight junction protein family, has been reported to be a predictor of recurrence after hepatectomy (5). We performed immunohistochemistry (IHC) for claudin-10 in tissues obtained from the 12 patients who underwent resection and compared the staining patterns with CT enhancement patterns.

Materials and methods

Of the 57 patients with HCC treated at Saiseikai-kure Hospital during the period of January 1999 to December 2005, 12 were selected for this study based on the following criteria: i) the patient had undergone curative resection, ii) the patient had a mass >2 cm in diameter without intrahepatic metastasis, iii) the patient did not receive preoperative chemotherapy or chemoembolization, and iv) the patient had preserved liver

Correspondence to: Dr Kazuhiro Yoshida, Department of Surgical Oncology, Research Institution for Radiation Biology and Medicine, Hiroshima University, 1-2-3 Kasumi, Minami-ku, Hiroshima 734-8551, Japan
E-mail: kyoshida@hiroshima-u.ac.jp

Key words: hepatocellular carcinoma, claudin-10

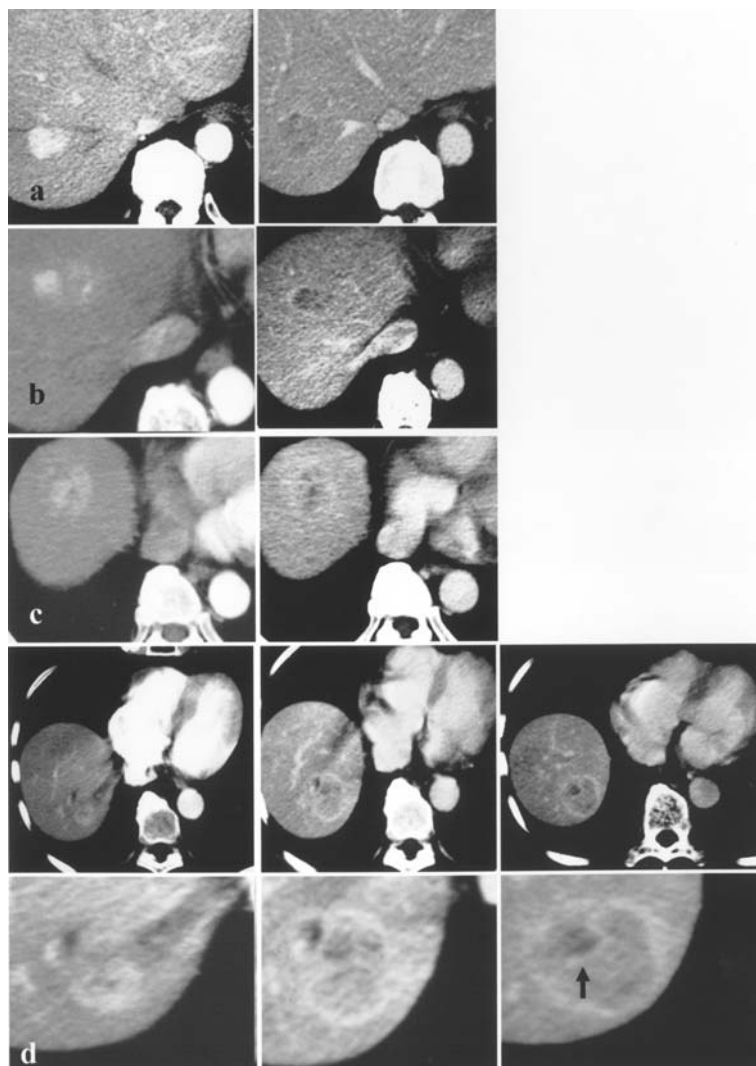


Figure 1. Representative dynamic computed tomography (CT) images. Early-phase images are shown in the left column, and late-phase are shown in the right column (a-c). Early-phase images are shown on the left, late- and equilibrium-phase images are shown in the center and right, respectively (d). (a) Type I tumor showed an area of homogenous hyperenhancement in the early phase and an area of hypoenhancement due to washout of contrast medium in the late phase (case 3). (b) Type II tumor showed an area of hyperenhancement in the early phase and an area of delayed enhancement in the late phase (case 5). (c) Type III tumor showed an area of hyperenhancement in the early phase, an area of delayed enhancement in the late phase and an area of hypoenhancement in all phases [(c), case 7; (d), case 11]. At the boundary of each area, fibrous septa were visible in the equilibrium phase (d, arrow).

function (Child-Pugh A). Subjects were 10 men and 2 women with a mean age of 68 years. Serologic testing showed that 6 patients were positive for hepatitis C virus antibody, and 1 was positive for hepatitis B surface antigen. Three patients suffered from alcoholic liver disease. The remaining 2 patients had autoimmune hepatitis and non-alcoholic steatohepatitis, respectively. Serum α -fetoprotein and vitamin K antagonist II levels were increased in 3 of 12 patients and in 1 of the 6 patients, respectively. Preoperative diagnosis was made on the basis of clinical features and CT findings. CT (Highspeed Advantage SG, GE, USA) was performed according to the following protocol. After unenhanced CT scanning, 50 ml of iopamidol (Iopamiron 300, Nihon Schering, Osaka, Japan) was injected at 2-4 ml/sec by means of a power injector. CT scanning was started 30-40 sec after injection (early phase). Late-phase images were obtained 4-6 min after injection.

All of the 12 patients underwent subsegmentectomy. Macroscopic classification of the tumor was performed according to Kanai's classification: 1, single-nodular type

(roughly round tumor with clear demarcation); 2, single-nodular type with extranodular growth; and 3, contiguous multinodular-type (tumor formed by a cluster of small and contiguous nodules). The cut surface was parallel to the scanning axis.

Resected specimens were fixed in formalin, embedded in paraffin and sectioned. Sections were stained with hematoxylin and eosin. Histologic subtype was determined according to the general rules for the clinical and pathologic study of primary liver cancer of the Liver Cancer Study Group of Japan. If a tumor showed more than two histologic grades, a predominant form was determined. Histologic grade was compared to CT findings in each case. Histopathologic examination included assessment of the non-tumorous liver parenchyma and the presence of vascular invasion.

The presence and location of recurrence after hepatectomy were assessed. We could not assess survival rate because of the small number of cases. Thus, we performed IHC for claudin-10. IHC for claudin-10 was carried out with a rabbit polyclonal anti-claudin-10 antibody (1:50, ab24792.,

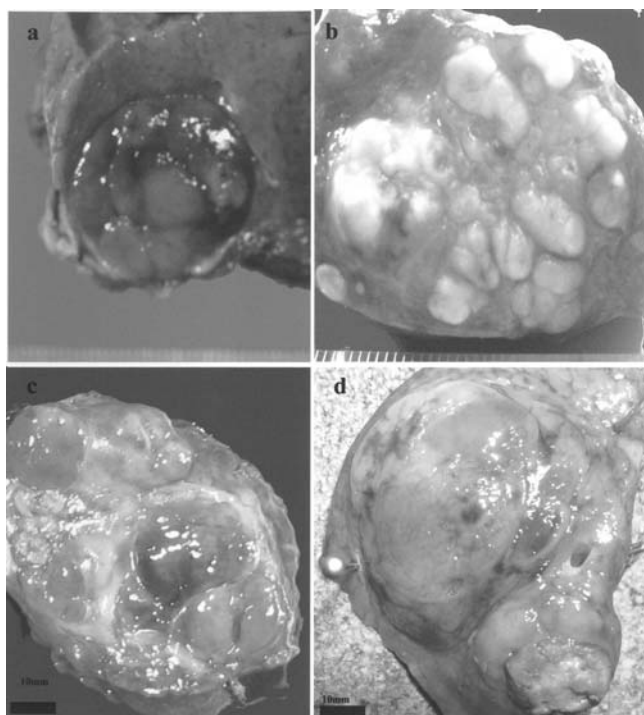


Figure 2. Representative macroscopic images of resected specimens. (a) Of the six type I tumors, four were single nodular, composed of homogenous soft tan tissue with regular margins (case 3). (b) The remaining two type I cases were multinodular, comprising yellowish tissue divided by fibrous septa. Each nodule showed similar gross morphology (case 1). (c) Type II tumors comprised soft tan tissue intermingled with white fibrous tissue (case 5). (d) Type III tumors were multinodular, comprising soft tan tissue with bile production, yellowish fatty tissue and firm white tissue with necrosis. Fibrous septa were visible at the boundary of each area.

Abcam Ltd., Cambridge, UK). The Dako LSAB kit (Dako, Carpinteria, CA, USA) was used for IHC. Paraffin-embedded sections were deparaffinized in xylene, rehydrated through graded ethanol series and microwaved in citrate buffer for 15 min to retrieve antigenicity. After endogenous peroxidase activity was blocked with 3% H₂O₂-methanol for 10 min, sections were incubated with primary antibody for 8 h at 4°C, followed by sequential 10-min incubations with biotinylated anti-rabbit IgG and peroxidase-labeled streptavidin. Staining was completed after a 10-min incubation with the substrate-chromogen solution. Sections were counterstained with 0.1% hematoxylin. Results of antibody staining were graded according to the percentage of stained target cells. Staining was considered positive if at least 25% of the cells were stained. Positivity was determined specifically in vascularly invasive lesions.

Results

Dynamic CT findings. Dynamic CT findings were classified into three types on the basis of differences in enhancement patterns (Fig. 1). Type I tumors (n=6) appeared as an area of homogeneous hyperenhancement in the early phase, followed by hypoenhancement due to the washout of contrast medium in the late phase (high-low), which is characteristic of HCC. Type II tumors (n=2) appeared as an area of hyperenhancement in the early phase and of delayed enhancement in the late

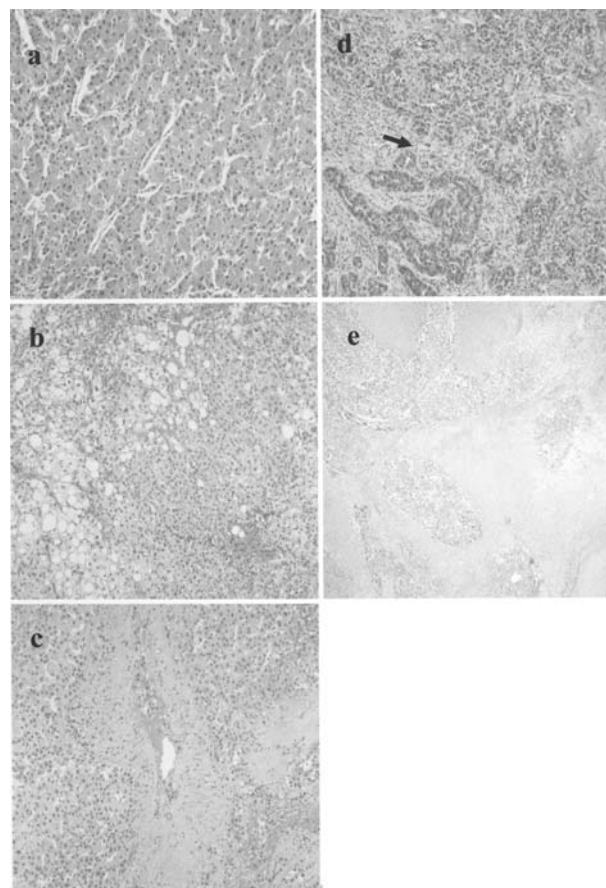


Figure 3. Representative histopathologic images of type I and II tumors. Original magnification is x100 unless otherwise stated. (a) In type I tumor, cells exhibited a thick trabecular pattern with several layers of moderately differentiated HCC. (b) In one case of type I tumor, a gradual transition from well-differentiated HCC accompanied by fatty change to moderately differentiated HCC was visible (case 9). (c) In two cases of type I tumor, fibrous septa divided similar moderately differentiated HCCs (case 3). (d) Combined hepatocellular-cholangiocarcinoma (case 5, type II). Moderately differentiated HCC with a trabecular pattern is shown on the right side, and cholangiocarcinoma with a tubular pattern is shown on the left side. The two components exhibited a gradual transition (arrow). (e) Scirrhus HCC (case 4, type II). Sinusoidal blood spaces were replaced by dense fibrous bands, and tumor trabeculae were atrophic. Magnification, x40.

phase (low-high). In type II tumors, the two components could be differentiated distinctly. Type III tumors (n=4) showed an intricate enhancement pattern. Tumors comprised an area of hyperenhancement in the early phase, an area of delayed enhancement in the late phase, and an area of hypoenhancement in all phases (low-low). In addition, linear enhancement was observed at the boundary of each area in the equilibrium phase.

Gross appearance. Four type I tumors (cases 1, 2, 6 and 8) appeared as single nodules comprising homogeneous soft tan tissue (Fig. 2a). The remaining two tumors (cases 3 and 9) were multinodular, in which homogeneous yellowish dense tissue was divided by thin to thick fibrous septa (Fig. 2b). Type II tumors (cases 4 and 5) were multinodular comprising soft tan tissue intermingled with firm white tissue (Fig. 2c). Type III tumors (cases 7 and 10-12) were multinodular (Fig. 2d), comprising soft tan tissue, yellowish fatty tissue, and white firm tissues with necrosis. Each component was divided by fibrous septa.

Table I. Clinicopathologic features of the 12 cases.

Case	Age/Sex	Background	AFP	PIVKA	Size	CT-type	Macro	V	NT
1	66/M	HCV	24	991.0	2.5	I	MN	+	LC
2	73/M	Alc	1988	*	4.8	I	SN	+	LC
3	70/M	HCV	5.0	12.0	2.2	I	SN	-	LC
4	81/M	AIHA	1209	20.0	7.0	II	MN	+	LC
5	60/M	HBV	5.0	*	5.0	II	MN	+	CH
6	58/M	HCV	13.5	*	6.0	I	SN	-	LC
7	61/M	HCV	4.8	*	2.5	III	MN	-	LC
8	77/M	Alc	109.2	*	2.8	I	SN	-	LC
9	70/M	HCV	14.6	13.0	2.5	I	MN	-	CH
10	72/F	NASH	15.0	7.0	2.8	III	MN	+	LF
11	65/M	HCV	8.4	10.0	2.8	III	MN	-	CH
12	63/F	Alc	11.0	*	3.5	III	MN	+	LC

M, male; F, female; Background, clinical background; HCV, hepatitis C infection; HBV, hepatitis B infection; Alc, alcoholic liver disease; AIHA, autoimmune hepatitis; NASH, non-alcoholic steatohepatitis; AFP, α -fetoprotein (ng/ml); PIVKA, vitamin K antagonist II (U/ml); Size, cm in diameter; CT-type, enhancement pattern on dynamic computed tomography, described in results section; SN, single nodular type; MN, multinodular type; V, presence of portal invasion; NT, pathologic features of non-tumorous liver parenchyma.

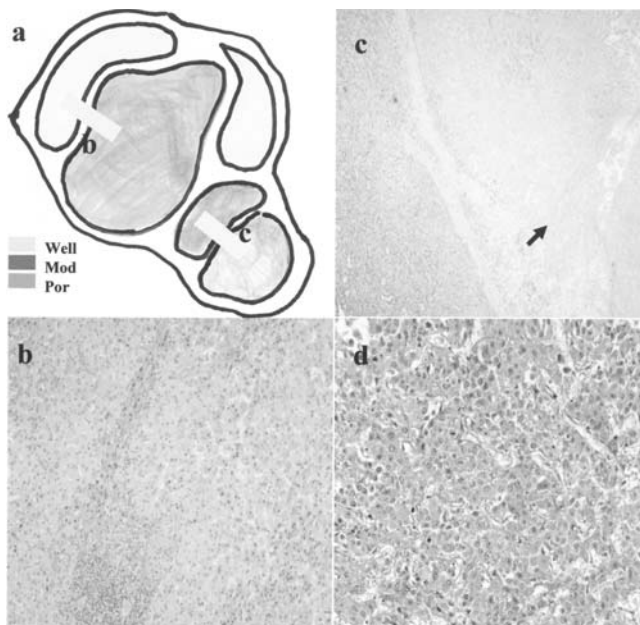


Figure 4. Representative microscopic features of type III tumors (case 11). (a) Schematic of the cut surface of the tumor. The distribution of histologic subtypes is indicated. (b) Well-differentiated HCC (left side) and moderately differentiated HCCs with trabecular pattern (right side) were divided by fibrous septa (original magnification x100). (c) Thick fibrous septa divided moderately differentiated HCC from poorly differentiated HCC. Poorly differentiated components included marked necrosis and fibrosis (arrow) (original magnification x40). (d) Poorly differentiated components showed a solid growth pattern with a slit-like blood space. Bizarre mononuclear cells are visible (original magnification x400).

Histologic features. Type I tumors consisted mainly of moderately differentiated HCC in a thick trabecular pattern (Fig. 3a), intermingling in part with well-differentiated HCC

Table II. Histology, prognosis and expression pattern of claudin-10.

Case	Histology	Rec	Prognosis	Claudin-10	
				T	Vp
1	Mod	5 (+)	22 A	-	-
2	Mod	(-)	64 D	-	-
3	Mod>Well	(-)	5 A	-	*
4	Scirrhus	(-)	64 A	-	-
5	Combined	(-)	6 A	+	+
6	Mod	(-)	17 A	-	*
7	Mod>Poor>Well	3 (+)	3 D	+	*
8	Mod	8 (+)	48 D	-	*
9	Mod	(-)	16 A	-	*
10	Poor>Mod	(-)	24 A	+	+
11	Mod>Poor>Well	3 (+)	4 A	+	*
12	Mod>Poor	5 (+)	8 A	+	+

Mod, moderately differentiated HCC; Well, well-differentiated HCC; Poor, poorly differentiated HCC; Rec, presence of recurrence of remnant liver and interval from hepatectomy; Prognosis, interval (months); A, alive; D, dead; Claudin-10, expression of claudin-10; T, tumorous components; Vp, portally invasive components.

showing a slight fatty change (Fig. 3b). In the two cases with fibrous septa (cases 3 and 9), each component divided by septa showed a similar histologic subtype (Fig. 3c). In type II tumors, one case (case 5) was combined hepatocellular-cholangiocarcinoma (Fig. 3d) and another (case 4) was

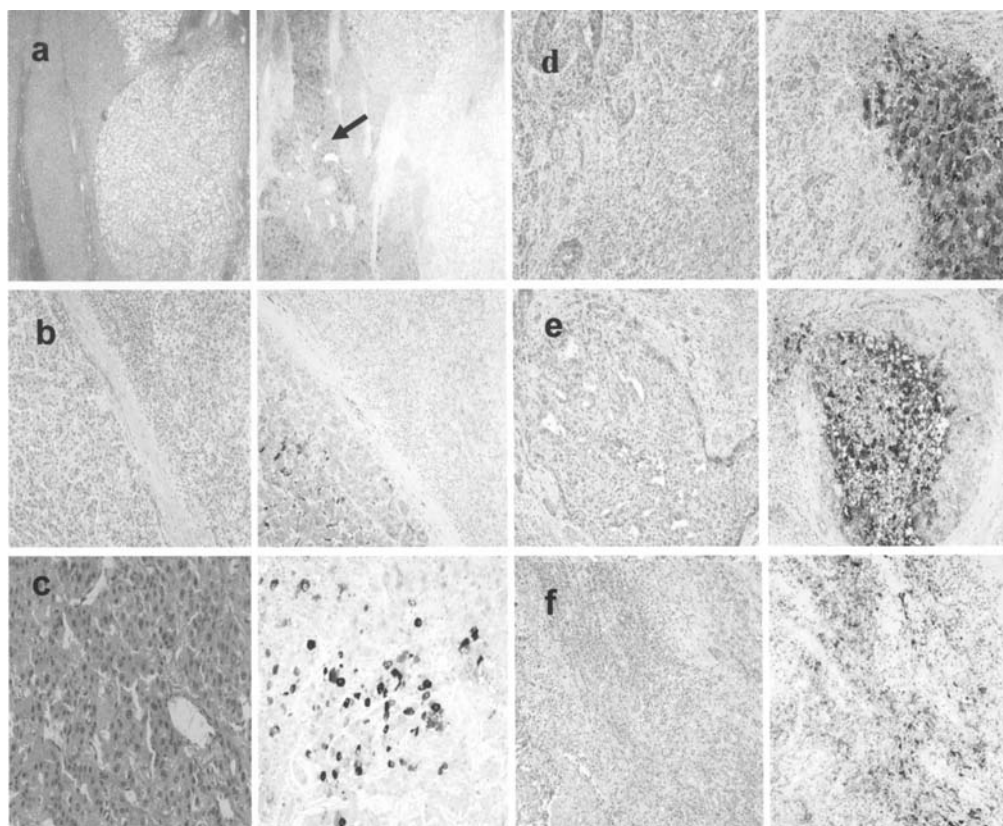


Figure 5. Immunostaining for claudin-10 in several HCC components. Original magnification is x100 unless otherwise stated. Representative hematoxylin and eosin-stained sections are shown in the left column and corresponding immunohistochemically stained sections are shown in the right column. (a) Well-differentiated HCC with fatty change showed no claudin-10 immunostaining (case 3). Corresponding cirrhotic liver parenchyma showed weak cytoplasmic immunostaining (arrow) (x40). (b) No claudin-10 immunostaining was observed in moderately differentiated HCC of type I tumors (case 1) (x40). (c) HCC components of combined hepatocellular-cholangiocarcinoma showed strong claudin-10 immunostaining. (d) Claudin-10 immunostaining was localized in the cytoplasm, with granular staining around nuclei (case 5) (x400). (e) Vascular invasive lesions of type III tumors showed strong claudin-10 immunostaining (case 11). (f) Claudin-10 immunostaining was focally positive in poorly differentiated components of type III tumor (case 11).

scirrhous HCC (Fig. 3e). Type III tumors were composed of well, moderately (Fig. 4b), and poorly (Fig. 4c and d) differentiated HCC. Well-differentiated HCC components were accompanied by fatty change and moderately differentiated components showed a thick trabecular pattern. Poorly differentiated components were accompanied by marked fibrosis and necrosis (Fig. 4c arrow, arrowhead). Each component was divided by fibrous septa (Fig. 4b and c).

Outcome and claudin-10 IHC findings are shown in Table II. Because of the small number of cases, sufficient analysis of prognosis could not be performed. In type III tumors, 3 of the 4 patients suffered recurrence in the remnant liver within six months after surgery.

Claudin-10 immunoreactivity was identified in 5 of the 12 cases, including 4 type III tumors and 1 combined hepatocellular-cholangiocarcinoma. Cirrhotic liver parenchyma showed faint homogeneous immunostaining (Fig. 5a and b). In type III tumors, moderately and poorly differentiated HCC cells showed strong cytoplasmic claudin-10 immunostaining (Fig. 5f). Staining was heterogenous and often localized around the nuclei (Fig. 5d). In addition, strong expression was observed in the vascularly invasive lesions of type III tumors (Fig. 5e). In combined hepatocellular-cholangiocarcinoma, staining was observed only in the HCC component (Fig. 5c).

Discussion

In the present study, three CT enhancement patterns were identified in the 12 cases of resected HCC of up to 2 cm in diameter. Type I was defined as a pattern of hyperenhancement throughout the tumor in the early phase, fading to hypoenhancement in the late phase (high-low), a finding characteristic of HCC. Type II tumors appeared as an area of hyperenhancement in the early phase (high-low) and an area of hyperenhancement in the late phase (low-high). Histologically, type II tumors were considered unusual, and included combined hepatocellular-cholangiocarcinoma, and scirrhous HCC. We believe that areas showing hyperenhancement in the early phase correspond to moderately differentiated HCC components and that the areas showing hyperenhancement in the late phase correspond to abundant fibrous stroma (6). In type III tumors, high-low, low-high and low-low components were observed. Histologically, high-low components corresponded to moderately or poorly differentiated HCC, and low-high components corresponded to fibrosis. Low-low components corresponded to poorly differentiated HCC with marked necrosis or to well-differentiated HCC. Each component was divided by thick fibrous septa, and the cut surface of the tumor was multinodular. The pathologic features of type III tumor could be summarized as follows: i)

gross appearance is multinodular; ii) each nodule shows a different histologic pattern of differentiation; iii) tumors are accompanied by marked necrosis and fibrosis surrounding components of poorly differentiated HCC. Interestingly, three of the four type III patients developed recurrence in the residual liver within 6 months after hepatectomy.

The classification of HCC is based on gross patterns of tumor growth and spread. The gross appearance of multinodular type may reflect the emergence of cellular populations with higher proliferative and invasive activity. Some investigators have reported that multinodular-type HCC is associated with increased risk of HCC recurrence after surgical treatment (2,3) However, the Liver Cancer Study Group of Japan stated that macroscopic subtypes are not associated with prognosis or recurrence after hepatectomy. To confirm whether gross classification can be a predictive factor for recurrence and prognosis, large-scale studies are necessary.

In the present study, two of the six type I cases showed multinodular morphology similar to that of type III cases. However, CT showed a homogeneous high-low pattern (type I) in these two cases, and thus we preoperatively diagnosed single nodular type. This discrepancy may be due to the following: i) in these two cases, each nodule showed similar histologic morphology of moderately differentiated HCC in a thick trabecular pattern; ii) fibrous septa was not visible due to the lack of equilibrium-phase images obtained 10-15 min after injection. Hui *et al* reported that the rate of correct diagnosis of macroscopic subtype by CT is 46% (2). To overcome this problem, assessment in the equilibrium phase may be useful. In addition, the two type I cases of multinodular type did not show recurrence during the follow-up period. However, three of the four type III cases showed recurrence in the remnant liver. Type III tumors included poorly differentiated HCC. However, poorly differentiated HCC generally shows a high-low pattern (7). We observed a low-low pattern in poorly differentiated components, due to marked necrosis and fibrosis. We believe that type III tumors show various pathologic features including dedifferentiation, necrosis and fibrosis and exhibit more malignant behavior than do the other tumor types.

Alterations in several cancer-related genes, such as p53, Rb and p16^{INK4}, have been shown to be involved in HCC (4). We hypothesized that the genesis of the different gross, histologic and CT enhancement patterns, as observed in the present study, involves different molecular mechanisms. Recently, several proteins have been identified via microarray method as prognostic factors for HCC. Cheung *et al* reported that claudin-10, a member of claudin tight junction protein family, could be used as a molecular marker for disease recurrence after curative hepatectomy by quantitative RT-PCR with primary tumor tissues (5). To determine whether type III tumors have greater malignant potential, we performed claudin-10 immunohistochemistry. Claudin-10 immunostaining was observed in five of the 12 cases. Of the five positive cases, four were type III and one was HCC components of combined

hepatocellular-cholangiocarcinoma. Staining was cytoplasmic and was localized in part around nuclei. These results support our hypothesis. The biologic function of claudin-10 is unknown. Several claudins, including claudin-1, -2, -4, and -7 have been reported to be overexpressed in tumors (8-11). Generally, claudins are localized at the cell membrane because of their specific function involving tight junctions. However, in the present study, claudin-10 was localized in cytoplasm and often around nuclei. Notably, claudin-1 has been reported to be localized in the nuclei of cells in metastatic colorectal carcinoma lesions in the liver, whereas it has been reported to be localized at the cell membrane of mucosal epithelial components in primary colorectal carcinoma (8). In the present study, claudin-10 staining was strongly around the nuclei, particularly in vascularly invasive lesions of type III tumors. Thus, we believe that claudin-10 is involved in the metastatic invasion of HCC. The altered localization of claudin-10 may be explained by regulation by transcription factors or growth factors. Further functional analyses are necessary to elucidate the molecular mechanisms underlying the malignant potential of HCC. We conclude that type III tumors have greater malignant potential than do the other tumor types. Preoperative dynamic CT should be performed to assess and predict the histologic features and malignant potential of HCC.

References

1. Bruix J and Sherman M: Management of hepatocellular carcinoma. *Hepatology* 42: 1208-1236, 2005.
2. Hui AM, Takayama T, Sano K, *et al*: Predictive value of gross classification of hepatocellular carcinoma on recurrence after hepatectomy. *J Hepatol* 33: 975-979, 2000.
3. Inayoshi J, Ichida T, Sugitani S, *et al*: Gross appearance of hepatocellular carcinoma reflects E-cadherin expression and risk of early recurrence after surgical treatment. *J Gastroenterol Hepatol* 18: 673-677, 2003.
4. Laurent-Puig P and Zucman-Rossi J: Genetics of hepatocellular tumors. *Oncogene* 25: 3778-3786, 2006.
5. Cheung ST, Leung KL, Ip YC, *et al*: Claudin-10 expression level is associated with recurrence of primary hepatocellular carcinoma. *Clin Cancer Res* 15: 551-556, 2005.
6. Sanada Y, Shiozaki S, Aoki H, *et al*: A clinical study of 11 resected cases of combined hepatocellular-cholangiocarcinoma. Assessment of enhancement patterns on dynamics computed tomography before resection. *Hepatol Res* 32: 185-195, 2005.
7. Amano S, Ebara M, Yajima T, *et al*: Assessment of cancer cell differentiation in small hepatocellular carcinoma by computed tomography and magnetic resonance imaging. *J Gastroenterol Hepatol* 18: 273-279, 2003.
8. Dhawan P, Singh A, Deane NG, *et al*: Claudin-1 regulates cellular transformation and metastatic behavior in colon cancer. *J Clin Invest* 115: 1765-1776, 2005.
9. Amasheh S, Meiri N, Gitter AH, *et al*: Claudin-2 expression induces cation-selective channels in tight junctions of epithelial cells. *J Cell Sci* 115: 4969-4976, 2003.
10. Nichols LS, Ashfaq R and Iacobuzio-Donahue CA: Claudin-4 protein expression in primary and metastatic pancreatic cancer. *Am J Clin Pathol* 121: 678-684, 2001.
11. Kominsky SL, Argani P, Korz D, *et al*: Loss of the tight junction protein claudin-7 correlates with histological grade in both ductal carcinoma *in situ* and invasive ductal carcinoma of the breast. *Oncogene* 22: 2021-2033, 2003.